

# Magnetic phase diagram of cuprates and universal scaling laws

Yves Noat,<sup>1</sup> Alain Mauger,<sup>2</sup> and William Sacks\*<sup>2,3</sup>

<sup>1</sup>*Institut des Nanosciences de Paris, CNRS, UMR 7588*

*Sorbonne Université, Faculté des Sciences et Ingénierie, 4 place Jussieu, 75005 Paris, France*

<sup>2</sup>*Institut de Minéralogie, de Physique des Matériaux et de Cosmochimie, CNRS, UMR 7590, Sorbonne Université, Faculté des Sciences et Ingénierie, 4 place Jussieu, 75005 Paris, France*

<sup>3</sup>*Research Institute for Interdisciplinary Science, Okayama University, Okayama 700-8530, Japan*

(Dated: 23 janvier 2025)

In this article we consider the magnetic field phase diagram of hole-doped high- $T_c$  cuprates, which has been given much less attention than the temperature diagram. In the framework of the *pairon model*, we show that the two characteristic energies, the pair binding energy (the gap  $\Delta_p$ ) and the condensation energy ( $\beta_c$ ) resulting from pair correlations, give rise to two major magnetic fields, the upper critical field  $B_{c2}$  and a second field,  $B_{pg}$ , associated with the pseudogap (PG). The latter implies a second length scale in addition to the coherence length, characteristic of incoherent pairs. Universal scaling laws for both  $B_{c2}$  and  $B_{pg}$  are derived :  $B_{c2}$  scales with the critical temperature,  $B_{c2}/T_c \simeq 1.65$  T/K, in agreement with many experiments, and  $B_{pg}$  has a similar scaling with respect to  $T^*$ . Finally, Fermi arcs centered on the nodal directions are predicted to appear as a function of magnetic field, an effect testable experimentally.

\*Corresponding author : william.sacks@sorbonne-universite.fr

PACS numbers: 74.72.h,74.20.Mn,74.20.Fg

## Introduction

Establishing the magnetic phase diagram as a function of doping is a key step to grasp the fundamental mechanisms underlying superconductivity in cuprates. Under an applied magnetic field, type II superconductors satisfy general properties. Vortices appear above the lower critical field,  $B_{c1}$ , and the typical size of the vortex core is the superconducting (SC) coherence length  $\xi_0$ . The latter is directly related to the upper critical field,  $B_{c2}$ , through the relation  $B_{c2} = \frac{\Phi_0}{2\pi\xi_0^2}$ , where  $\Phi_0 = h/(2e)$  is the magnetic flux quantum.

In cuprates the phase coherence length is in the nanometer range so that the upper critical field is often too large to be measured, in which case its estimation can be made using indirect extrapolation methods. Such is the case, for instance, for  $\text{YBa}_2\text{Cu}_3\text{O}_{7-\delta}$  (YBCO) or  $\text{Bi}_2\text{Sr}_2\text{CaCu}_2\text{O}_{8+\delta}$  (BSCCO). This experimental limitation might explain some of the discrepancies for  $B_{c2}$  obtained in different experiments.

The upper critical field has been deduced from the specific heat by different groups [1, 2] on  $\text{La}_{2-x}\text{Sr}_x\text{CuO}_4$  (LSCO) for different hole concentrations ( $p$ ) from underdoped to overdoped sides of the critical  $T_c$  dome. The authors measured the dependence of the  $\gamma$  coefficient as a function of magnetic field, from which  $B_{c2}$  can be obtained. Their results indicate that  $B_{c2}$  follows a dome as a function of  $p$ , and hence follows the critical temperature. These findings are in qualitative agreement with the high-field measurements of the resistivity [3]. On the other hand, there is an apparent contradiction with experiments by Kato et al. [4], who estimate the upper critical field of  $\text{Bi}_{2+x}\text{Sr}_{2-x}\text{CaCu}_2\text{O}_{8+\delta}$  from the measured irre-

versibility field. In this case,  $B_{c2}$  qualitatively follows a dome for small carrier concentrations, but then increases monotonically to high values in the overdoped regime. Therefore, in order to address these issues, it is important to clarify the key parameters, i.e. the characteristic energies, lengths, and magnetic fields of high- $T_c$  cuprates.

More than 30 years after the discovery of cuprates by Bednorz and Müller [5], key questions such as the pairing ‘glue’, the nature of the pseudogap, and the role of the gap parameter, remain open issues. Above  $T_c$ , contrary to conventional superconductors, the normal metallic state is not recovered. Instead, the pseudogap (PG) state is found, characterized by a lowering of the quasiparticle DOS, which persists up to the higher temperature  $T^*$  [6].

In the BCS theory, the energy gap is proportional to the critical temperature :  $2\Delta/(k_B T_c) \simeq 3.52$ . The situation is different in cuprates since the amplitude of the gap is not directly related to  $T_c$ . A gap of the same order of magnitude persists above  $T_c$  [7] as well as within the vortex core, see Fig. 1, panel (a). This is confirmed by scanning tunneling spectroscopy (STS) measurements in disordered BSCCO thin films [8]. In the SC state, the quasiparticle spectrum displays the peak-dip structure. Crossing to the non-SC region, the coherence peaks disappear while the gap is preserved having roughly the same magnitude, see Fig. 1, panel (d). A similar transition is also observed as a function of temperature [7]. Therefore, since a gap exists even when the superfluid density vanishes, it cannot be the order parameter.

This conclusion is confirmed by the dependence of the energy gap with doping. In fact, the gap, which is directly measured by tunneling or photoemission spectroscopy, decreases linearly as a function of carrier density [9–11]. In the underdoped regime,  $T_c(p)$  has the opposite

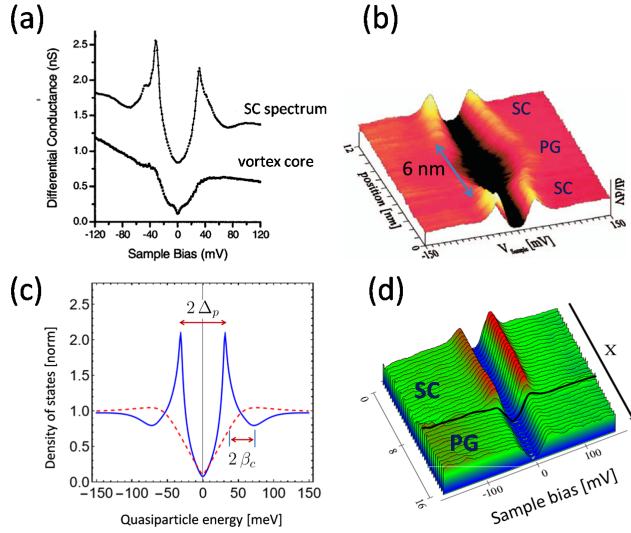


FIGURE 1. (Color online) Strong experimental evidence of the pseudogap (PG) state obtained when SC coherence is lost at *low temperatures*. In contrast to the conventional case, this PG state consists of incoherent pairons, even at the local scale[18]. a) STS spectrum taken at low temperature in the SC state as well as within the vortex core (adapted from [12]). b) STS spectra taken along a line crossing a vortex (adapted from [13]). c) Theoretical spectra (solid blue line) in the SC state and in the incoherent pseudogap state, red dashed line (adapted from [14–16]). d) STS spectra along a line crossing from an ordered region to a disordered region (adapted from [8]). All panels correspond to BSCCO(2212).

behavior with respect to the energy gap since it *increases* with doping. Two undecided questions thus emerge from these considerations :

1. What is the order parameter in cuprates ?
2. What is the magnetic phase diagram and its connection to the temperature phase diagram ?

In this article, we establish important physical parameters of hole-doped cuprates in the framework of the pairon model. Based on a two–fluid Ginzburg-Landau approach, we obtain the expressions for the characteristic lengths and magnetic fields. This allows to deduce the magnetic phase diagram of cuprates, and to compare it with the analogous temperature diagram.

### Characteristic energy scales of cuprates

In order to answer the above questions, we consider the pairon model wherein the SC state is the result of the condensation of preformed pairs due to their mutual interaction [17–19]. Once SC coherence is lost due to a magnetic field or rising temperature, the system becomes a ‘glassy’ PG state of incoherent pairons, such as in the vortex core. The corresponding phase diagram for hole-doped cuprates can then be described by two energy

scales : the pairing energy gap  $\Delta_p$  and the condensation (or correlation energy)  $\beta_c$ .

The meanings of  $\Delta_p$  and  $\beta_c$  in the pairon model are distinct. Pairons are bound holes on adjacent copper sites which form below  $T^*$  as a result of their local antiferromagnetic environment on the scale of  $\xi_{AF}$ , the AF correlation length [18]. They condense into a superconducting state at the critical temperature  $T_c$  ( $T_c \leq T^*$ ), forming a collective pairon state. The energy (per pairon) in the pseudogap state and in the SC state are respectively :

$$E_{pg} = -\Delta_p \quad (1)$$

$$E_{SC} = -\Delta_p - \beta_c \quad (2)$$

It is important to note that the condensation energy  $\beta_c$  is due to correlations between pairons. In a sense it is a ‘hidden’ term since, contrary to conventional superconductors, it does not correspond to a binding energy and is not measured as a usual gap in photoemission or scanning tunneling spectroscopy. However the coherence energy,  $\beta_c$ , is present in the quasiparticle spectrum for energies just above the coherence peak characterized by a sharp dip, see Fig. 1(c). The precise analysis of the quasiparticle spectra using a gap function  $\Delta(E_k)$  reveals quantitatively both energies  $\Delta_p$  and  $\beta_c$  [15–17].

We have previously shown that both  $\Delta_p$  and  $\beta_c$  are proportional to the same fundamental physical parameter, the effective exchange energy  $J_{eff}$  in the CuO plane. Note that  $J_{eff}$  is material dependent since it varies as a function of the  $c$ -axis coupling between CuO planes. This can explain the variations of  $T_c$  between different materials.

As a result of topological constraints of holes in the CuO plane [19], the following relations are derived for  $\Delta_p$  and  $\beta_c$  as a function of the hole concentration :

$$\Delta_p = J_{eff}(1 - p') \quad (3)$$

$$\beta_c = J_{eff}p'(1 - p') \quad (4)$$

Here  $p' = (p - p_{min}) / (p_{max} - p_{min})$  is the reduced density, with  $p_{min} = 0.05$  and  $p_{max} = 0.27$ . Thus,  $p'$  conveniently ranges from 0 to 1, from the start to end of the  $T_c$  dome. Moreover, the energy and temperature scales are linked by the relations [18] :

$$\Delta_p = 2.2 k_B T^* \quad (5)$$

$$\beta_c = 2.2 k_B T_c \quad (6)$$

Considering the available data on BSCCO(2212), the numerical factor does have some uncertainty :  $\sim 2.25 \pm .05$ . The simplest ratio of the two energies therefore leads to :

$$\frac{\beta_c}{\Delta_p} = \frac{T_c}{T^*} = p' \quad (7)$$

For LSCO this ratio is slightly lower ( $\approx 0.8 p'$ ) due to the relatively smaller  $T_c$ . As shown in a previous article [20], this ratio also determines the size of the Fermi arcs at the critical temperature.

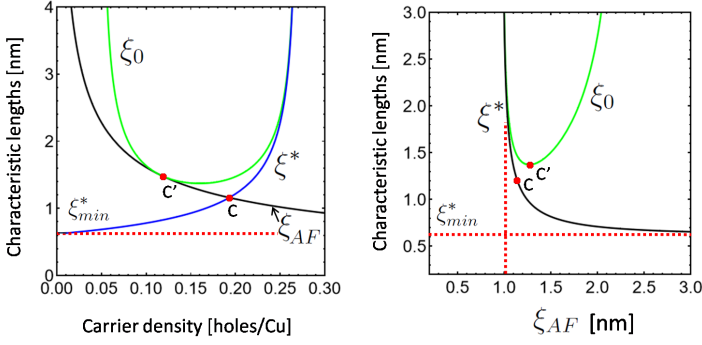


FIGURE 2. (Color online) Plot of the coherence length  $\xi_0$ , the pair correlation length  $\xi^*$ , and the antiferromagnetic correlation length  $\xi_{AF}$ , according to the model. a) All three lengths plotted as a function of carrier concentration. b)  $\xi_0$ ,  $\xi^*$  plotted as a function of  $\xi_{AF}$ . We note the special points  $c'$  and  $c$ , at the values  $p \simeq .12$ , and  $p \simeq .19$ , respectively. The plots are appropriate for BSCCO(2212).

### Characteristic lengths

A two-fluid model is a convenient way to derive the appropriate length scales. In order to describe the two different fluids, the superfluid (the coherent pairons of the condensate) and the fluid of incoherent pairons (pairons excited out of the condensate), we consider two coupled Ginzburg-Landau equations in zero applied field :

$$-\frac{\hbar^2}{2m}\nabla^2\psi_c + a\psi_c + b|\psi_c|^2\psi_c = 0 \quad (\text{condensate}) \quad (8)$$

$$-\frac{\hbar^2}{2m}\nabla^2\psi_{ex} + \bar{a}\psi_{ex} + \bar{b}|\psi_{ex}|^2\psi_{ex} = 0 \quad (\text{excited pairs}) \quad (9)$$

Here  $|\psi_c|^2 = n_s$  is the condensate density and  $|\psi_{ex}|^2 = n_{ex}$  is the excited pairs density. For example, qualitatively, the condensate density  $n_s$  gives rise to the typical STS spectrum outside the vortex, whereas  $n_{ex}$  aptly describes the local density within the core (see Fig. 1 (b)).

Neglecting pair-breaking below  $T_c$  and phase fluctuations above  $T_c$ , the conditions that  $n_s(T) + n_{ex}(T) = n_0$  for  $T \leq T_c$  and  $n_s(T) = 0$  for  $T \geq T_c$  should be fulfilled. The variation of the free energy between the normal state and superconducting state (assuming  $T = 0$ ) is

$$\Delta F = \frac{a^2}{2b} = \frac{1}{2}n_s|a| \quad (10)$$

$$= \frac{1}{2}p'|a| \quad (11)$$

In addition, we have  $|\psi_c|^2 = n_s(T) = |a|/b$ . This allows to compare to the expression of  $\Delta F = \frac{1}{2}\beta_c p'$  expected in the pairon model, from which we deduce that  $|a| = \beta_c$ . Including pair-breaking below  $T_c$ , relevant to the highly-overdoped regime, gives the same result.

We therefore obtain the two length scales  $\xi_i = \sqrt{\frac{\hbar^2}{2mE_i}}$ , with  $i = 1, 2$ , associated with the two energies  $E_1 = \Delta_p$  and  $E_2 = |a| = \beta_c$  :

$$\xi^* = \sqrt{\frac{\hbar^2}{2m\Delta_p}} \quad (12)$$

$$\xi_0 = \sqrt{\frac{\hbar^2}{2m\beta_c}} \quad (13)$$

Here  $\xi^*$  is the length associated with the pairing gap while  $\xi_0$  is the coherence length associated with superconducting phase coherence.

A third important length scale is the antiferromagnetic correlation length and its dependence on the hole carriers,  $\xi_{AF}(p)$ . In a simple approach [18], we proposed that  $\xi_{AF}(p)$  is determined by the mean pairon-pairon distance in the CuO plane :

$$\xi_{AF}(p) = a_0\sqrt{\frac{2}{p}} \quad (14)$$

where  $a_0$  is the in-plane Cu-Cu distance. This formula is in qualitative agreement with neutron experiments [21]. In this picture, a given pairon is surrounded by an area, a Voronoi cell, corresponding to a well-defined AF magnetic order on the scale of  $\xi_{AF}(p)$ . In [18], we showed that the pairon binding energy,  $\Delta_p$ , is proportional to the Voronoi cell area, providing a simple explanation for its  $p$ -dependence.

It is instructive to see that, after a little algebra, two of the length scales  $\xi^*$  and  $\xi_{AF}(p)$  are connected by a simple equation :

$$\left(\frac{\xi_{min}^*}{\xi^*}\right)^2 + \left(\frac{\xi_{AF}^{min}}{\xi_{AF}}\right)^2 = 1 \quad (15)$$

where  $\xi_{min}^*$  is the value of  $\xi^*$  extrapolated to  $p = 0$ , and  $\xi_{AF}^{min} = \xi_{AF}(.27)$ . The above equation can be represented by a hyperbola (solid black line Fig. 2, right panel). The third length,  $\xi_0$ , can be conveniently expressed as :

$$\xi_0 = \frac{1}{\sqrt{p'}}\xi^*$$

The variation of the three length scales  $\xi_0$ ,  $\xi^*$  and  $\xi_{AF}$  as a function of carrier concentration are shown in Fig. 2, left panel. As seen in the figure, there is a striking difference in the behavior of  $\xi_0$  and  $\xi^*$ . In the highly underdoped regime  $\xi_0 \gg \xi^*$ , evidently the pairons behave dominantly as bosons. However, in the overdoped regime, i.e. towards the end of the  $T_c$ -dome,  $\xi_0 \rightarrow \xi^*$  as  $p \rightarrow p_{max}$ , so the two length scales approach each other asymptotically. At the same time, as can be seen using eqns. (3) and (4), close to the critical point  $p = p_{max}$  or  $p' = 1$ , the associated energy scales  $\Delta_p$  and  $\beta_c$ , also approach each other, and vanish identically in the limit  $p \rightarrow p_{max}$ .

The overdoped side of the dome thus recalls the BCS case where the coherence length is determined by the

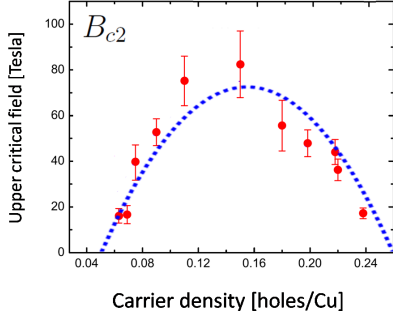


FIGURE 3. (Color online) Upper critical field,  $B_{c2}$ , for LSCO as a function of carrier density. Experimental values (red points) are taken from Wang et H.-H. Wen [1]. Dashed blue line : theoretical prediction from the model.

energy gap. However, it would be misleading to conclude that one recovers the BCS mechanism in this regime. Indeed, the underdoped and overdoped regimes clearly correspond to different limits, given by the ratio  $\xi_0/\xi^*$ . However, the mechanism at the heart of the cuprate SC coherence is imposed by the conjunction of the geometrical constraints of the CuO plane and the finite size of hole-pairs [19]. Detailed considerations of the model confirm that pairons, i.e. two holes bound on neighboring copper sites in an antiferromagnetic environment, are the fundamental quantum objects across the  $T_c$ -dome.

To conclude this discussion, we note that two special points in the phase diagram exist :  $c'$  and  $c$  (respectively, at the concentrations  $p \simeq .12$  and  $p \simeq .19$ ), see Fig. 2. These two points correspond to the common tangent of  $\xi_{AF}$  with  $\xi_0$  and the intersection of  $\xi_{AF}$  with  $\xi^*$ , respectively. We see the further condition that  $\xi_{AF}(p) \leq \xi_0(p)$  for all  $p$ , and that  $c'$  (at  $p \simeq .19$ ) is an evident transition point involving the the characteristic length  $\xi^*$ . The latter phenomenon will be tackled in a future report.

### Characteristic magnetic fields of cuprates

The coherence length  $\xi_0$ , is the typical size of the vortex core and it is associated with the upper critical field  $B_{c2}$ . Similarly,  $\xi^*$  is associated with a higher field  $B_{pg}$  reflecting the pseudogap state. While  $B_{c2}$  is the field necessary to destroy SC phase coherence, we shall show that pairons theoretically survive up to  $B_{pg} > B_{c2}$ .

From the two length scales, one can deduce the expressions of the two important magnetic fields using the relations :

$$B_{c2} = \frac{\Phi_0}{2\pi\xi_0^2} \quad (16)$$

$$B_{pg} = \frac{\Phi_0}{2\pi\xi^{*2}} \quad (17)$$

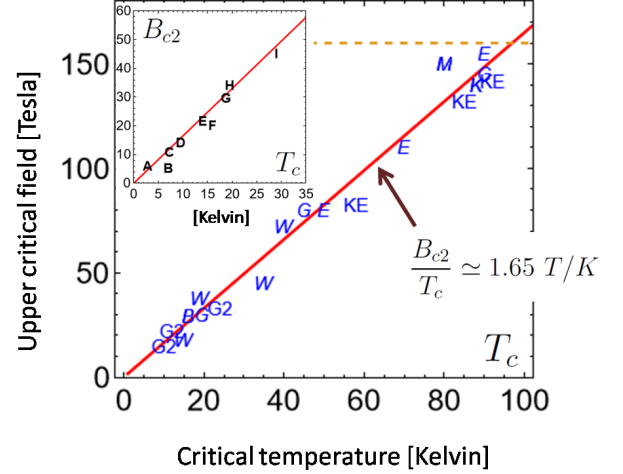


FIGURE 4. (Color online) Upper critical field,  $B_{c2}$ , as a function of the critical temperature,  $T_c$ , for different cuprate materials and doping values. Inset : Similar plot for conventional superconductors A to H,  $B_{c2}$  follows a similar line with  $B_{c2}/T_c \simeq 1.7$  T/K.

In the main plot : KE : Krusin Elbaum et al. BSCCO [22], K : Kugler et al. BSCCO [13], M : Maggio Aprile et al. YBCO [23], W : Wang et Wen LSCO [1], G : Grisonnanche et al. YBCO [3], G2 : Grisonnanche et al. Tl2201 [3].

Details for the inset :

A : BaBi<sub>3</sub> [24], B : NbSe<sub>2</sub> [25],[26], C : MgCNi<sub>3</sub> [27], D : NbTi [28], E : V<sub>3</sub>Ga [29], F : V<sub>3</sub>Si [30, 31], G : Nb<sub>3</sub>Sn [30], H : Nb<sub>3</sub>Al [32], I : Rb<sub>3</sub>C<sub>60</sub>[33].

Replacing the expressions for  $\xi_0$  and  $\xi^*$ , we obtain :

$$B_{c2} = \left( \frac{m\Phi_0}{\pi\hbar^2} \right) \beta_c \quad (18)$$

$$B_{pg} = \left( \frac{m\Phi_0}{\pi\hbar^2} \right) \Delta_p \quad (19)$$

One first important consequence from Eq. (18) is that the upper critical field must follow the superconducting dome. This is in good agreement with the findings of Wang and Wen [1], as shown in Fig. 3.

One can therefore deduce important scaling relations. Since the upper critical field in the pairon model is proportional to the coherence energy  $\beta_c$ , we have :

$$\frac{B_{c2}}{\beta_c} = \frac{m\Phi_0}{\pi\hbar^2} = \mathcal{C} = \text{universal constant} \quad (20)$$

where  $\mathcal{C} \simeq 8.6$  T/meV. Using  $\beta_c = 2.25 k_B T_c$ , it follows that :

$$\frac{B_{c2}}{T_c} \simeq 1.65 \text{ T/K} \quad (21)$$

This relation should hold for any hole-doped cuprate and for arbitrary carrier concentrations within the SC range. In Fig. 4, we have plotted the upper critical field for several materials and doping values. The agreement confirms the linear relation between  $B_{c2}$  and  $T_c$ . We note that a

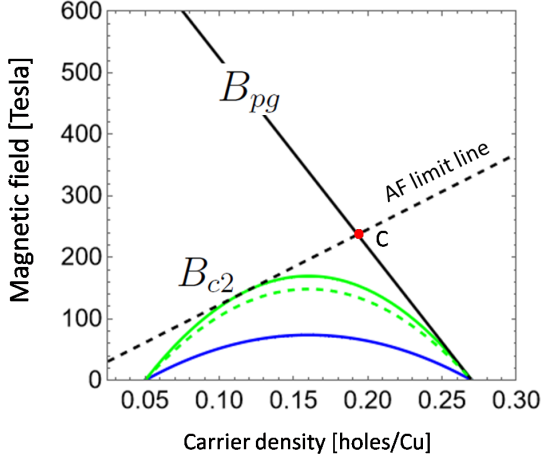


FIGURE 5. (Color online) Magnetic phase diagram showing the two main characteristic fields, the upper critical field  $B_{c2}$  and the field associated with pseudogap  $B_{pg}$  (solid black line). Dashed green line :  $B_{c2}(p)$  deduced using the estimated value of the coherence length from the vortex core in BSCCO (Fig.1, panel (b)). Solid green line :  $B_{c2}(p)$  of BSCCO using the theoretical value for  $\beta_c$ . Solid blue line :  $B_{c2}(p)$  predicted for LSCO. Dashed black line : upper limit for  $B_{c2}(p)$  in the model (associated with the length scale  $\xi_{AF}$ ). Note that pairons form below the pseudogap magnetic field,  $B_{pg}$ , and become coherent below  $B_{c2}$ .

wide variety of conventional superconductors follow a similar trend (inset of Fig. 4), however in this case each material has a fixed carrier concentration, in contrast to cuprates. Finally, using Eqs. (5) and (19), the model predicts a similar scaling of the pairing field with  $T^*$  :  $B_{pg}/T^* \simeq 1.65$  T/K.

### Magnetic phase diagram and discussion

The magnetic phase diagram thus appears to be very analogous to the temperature phase diagram. Pairons form below the pseudogap field  $B_{pg}$  and become coherent below  $B_{c2}$ , see Fig. 5. This is similar to the phase diagram proposed by Krusin-Elbaum et al. [22], based on high magnetic field c-axis resistivity measurements. The striking analogy between the temperature and magnetic phase diagrams suggests that the magnetic field and the temperature produce similar effects. Phase coherence is destroyed either by raising the temperature above  $T_c$ , or by applying a magnetic field stronger than  $B_{c2}$ , as in conventional superconductors. However, pairons survive in cuprates above  $T_c$  up to  $T^*$  and, as our work confirms, above  $B_{c2}$  up to  $B_{pg}$ . The interpretation of  $B_{pg}$  as the pair-breaking field is thus reasonable, whereas  $B_{c2}$  breaks the phase coherence, in clear agreement with experiment (Fig. 1).

A unique property of cuprates is the existence of Fermi arcs of ‘normal’ electrons centered around the nodal directions at finite  $T$  (see [6] and Refs. therein). In our

model hole pairons are associated with a continuum of electron Cooper pairs in momentum space. Four Fermi arcs then appear due to the weaker binding energy of Cooper pairs with momenta close to the nodal directions [20]. As shown using ARPES experiments [6], a given Fermi arc is very small at low temperature, in agreement with  $d$ -wave pairing. Then, as  $T \rightarrow T_c$ , the Fermi arcs grow monotonically with temperature, at a rate that is  $p$ -dependent. The complete Fermi surface is recovered at the higher temperature  $T^*$  [20].

To quantify the Fermi arc size using simple arguments, we recall that the  $d$ -wave pair potential is well approximated by :  $\Delta(\theta) = \Delta_p \cos(2\theta)$  where  $\theta$  is the momentum angle measured from the antinodal direction. Thus, at some finite temperature  $T \leq T_c$ , pairs whose energy satisfies  $\Delta_p \cos(2\theta) \leq 2.2 k_B T$  will decay into normal electron states around the node. The Fermi arc does indeed increase with temperature, an effect which is more pronounced for higher carrier concentrations. In particular, at  $T = T_c$  we obtain the critical angle  $\theta_c$  which characterizes the width ( $2\theta_c$ ) of the Fermi arc :

$$\cos(2\theta_c) = \frac{\beta_c}{\Delta_p} = \frac{T_c}{T^*} = p' \quad (22)$$

This critical angle has been directly measured by Hashimoto et al. [6] where, for near optimal doping, the above ratio is about 1/2 giving  $\theta_c \simeq 30^\circ$ . (As previously mentioned, the simple ratio above, valid for BSCCO-2212, would be slightly smaller for LSCO by about 20%.)

The same physical effect should also occur in a magnetic field. Indeed, using eqns. (18) and (19) we obtain the analogous relation for the critical angle :

$$\cos(2\theta_c) = \frac{B_{c2}}{B_{pg}} \quad (23)$$

Again, the complete Fermi surface is only recovered at the higher pairing field,  $B_{pg}$ . The existence of such Fermi arcs for the lower field,  $B \leq B_{c2}$ , can be considered a critical test for the pairon model.

### Conclusion

In conclusion, we have derived expressions for the length scales and magnetic fields of hole-doped cuprates. A two-fluid model, using two coupled Ginzburg-Landau equations, describes the condensate (the coherent pairs) and the incoherent pairs (pairs excited out of the condensate). The two energy scales describing cuprates, the energy gap,  $\Delta_p$ , and the condensation energy,  $\beta_c$ , give rise to two characteristic magnetic fields, the upper critical field,  $B_{c2}$ , and the pseudogap field,  $B_{pg}$ . The magnetic phase diagram is therefore very analogous to the temperature phase diagram. It appears that the same critical point,  $p = p_{max}$ , at the end of the  $T_c$  dome, also exists in the magnetic diagram.

In this work, we have established a universal scaling law for  $B_{c2}$  as a function of the critical temperature,  $B_{c2}/T_c \simeq 1.65 \text{ T/K}$ , in quantitative agreement with experiments, which should be valid for all cuprates on the hole-doped side, and for any carrier concentration. A similar scaling law is predicted for the pseudogap field,  $B_{pg}$ , but with respect to  $T^*$ .

Instead of a single coherence length  $\xi_0$ , the model invokes a second length,  $\xi^*$ , associated with the pairing gap. Their dependence on the carrier concentration, from underdoped to overdoped sides of the phase diagram, offers unique insights into the cuprate mechanism. The present theory can be used to express the thermodynamic field, the condensation energy, the lower critical field  $B_{c1}$ , and the London penetration depth  $\lambda$ , which we leave for a future report.

Finally, we propose that Fermi arcs should also exist as a function of magnetic field, a prediction that can be used as a strong experimental test of the model.

### Acknowledgements

The authors gratefully acknowledge discussions with Dr. Hiroshi Eisaki, Dr. Shigeyuki Ishida (AIST, Tsukuba), and Prof. Atsushi Fujimori (Tokyo University).

A.M. and W.S. acknowledge partial support from the French National Research Agency (ANR), project ‘Superstrong’ under contract no. ANR-22-CE30-0010 (Principal Investigator : Andrea Gauzzi).

W.S. is grateful for continual support of the RIIS Institute of Okayama University, Japan, to Prof. Takayoshi Yokoya (host), and his ‘visiting professor’ status while on leave from SU.

- 
- [1] Y. Wang and H.-H. Wen, Doping dependence of the upper critical field in  $\text{La}_{2-x}\text{Sr}_x\text{CuO}_4$  from specific heat, *Europhys. Lett.*, **81**, 57007 (2008).
  - [2] H. H. Wen, H. P. Yang, S. L. Li, X. H. Zeng, A. A. Soukiassian, W. D. Si and X. X. Xi, Hole doping dependence of the coherence length in  $\text{La}_{2-x}\text{Sr}_x\text{CuO}_4$  thin films, *Europhys. Lett.*, **64**, 790 (2003).
  - [3] G. Grissonnanche, O. Cyr-Choinière, F. Laliberté, S. René de Cotret, A. Juneau-Fecteau, S. Dufour-Beauséjour, M. -È. Delage, D. LeBoeuf, J. Chang, B. J. Ramshaw, D. A. Bonn, W. N. Hardy, R. Liang, S. Adachi, N. E. Hussey, B. Vignolle, C. Proust, M. Sutherland, S. Krämer, J. -H. Park, D. Graf, N. Doiron-Leyraud and Louis Taillefer, Direct measurement of the upper critical field in cuprate superconductors, *Nature Communications* **5**, Article number : 3280 (2014).
  - [4] Junichiro Kato, Shigeyuki Ishida, Tatsunori Okada, Shungo Nakagawa, Yutaro Mino, Yoichi Higashi, Takanari Kashiwagi, Satoshi Awaji, Akira Iyo, Hiraku Ogino, Yasunori Mawatari, Nao Takeshita, Yoshiyuki Yoshida, Hiroshi Eisaki, and Taichiro Nishio, Doping dependence of upper critical field of high- $T_c$  cuprate  $\text{Bi}_{2+x}\text{Sr}_{2-x}\text{CaCu}_2\text{O}_{8+\delta}$  estimated from irreversibility field at zero temperature, *J. Phys. Soc. Jpn.* **93**, 104705 (2024).
  - [5] J. G. Bednorz, K. A. Müller, Possible high  $T_c$  superconductivity in the Ba-La-Cu-O system, *Zeitschrift für Physik B Condensed Matter* **64**, 189 (1986).
  - [6] Makoto Hashimoto, Inna M. Vishik, Rui-Hua He, Thomas P. Devereaux and Zhi-Xun Shen, Energy gaps in high-transition-temperature cuprate superconductors, *Nature Physics* **10**, 483 (2014).
  - [7] Ch. Renner, B. Revaz, J.-Y. Genoud, K. Kadowaki, and ø. Fischer, Pseudogap precursor of the superconducting gap in under- and overdoped  $\text{Bi}_2\text{Sr}_2\text{CaCu}_2\text{O}_{8+\delta}$ , *Phys. Rev. Lett.* **80**, 149 (1998).
  - [8] T. Cren, D. Roditchev, W. Sacks, J. Klein, J.-B. Moussy, C. Deville-Cavellin, and M. Laguès, Influence of disorder on the local density of states in high- $T_c$  superconducting thin films, *Physical Review Letters* **84**, 147 (2000).
  - [9] Tohru Nakano, Naoki Momono, Migaku Oda, and Masayuki Ido, Correlation between the doping dependences of superconducting gap magnitude  $2\Delta_0$  and pseudogap temperature  $T^*$  in high- $T_c$  cuprates, *J. Phys. Soc. Jpn.* **67**, 2622-2625 (1998).
  - [10] S. Hüfner, M. A. Hossain, A. Damascelli, and G. A. Sawatzky, Two gaps make a high-temperature superconductor?, *Rep. Prog. Phys.*, **71**, 062501 (2008).
  - [11] N. Miyakawa, J. F. Zasadzinski, L. Ozyuzer, P. Gupta-sarma, D. G. Hinks, C. Kendziora, and K. E. Gray, Predominantly superconducting origin of large energy gaps in underdoped  $\text{Bi}_2\text{Sr}_2\text{CaCu}_2\text{O}_{8+\delta}$  from tunneling spectroscopy, *Phys. Rev. Lett.* **83**, 1018 (1999).
  - [12] S. H. Pan, E. W. Hudson, A. K. Gupta, K.-W. Ng, H. Eisaki, S. Uchida, and J. C. Davis, STM Studies of the Electronic Structure of Vortex Cores in  $\text{Bi}_2\text{Sr}_2\text{CaCu}_2\text{O}_{8+\delta}$ , *Phys. Rev. Lett.* **85**, 1536 (2000).
  - [13] Kugler, M., 2000, Ph.D. thesis, University of Geneva.
  - [14] Yves Noat Alain Mauger, William Sacks, Statistics of the cuprate pairon states on a square lattice, *Modelling Simul. Mater. Sci. Eng.* **31**, 075010 (2023).
  - [15] William Sacks, Alain Mauger and Yves Noat, Universal spectral signatures in pnictides and cuprates : the role of quasiparticle-pair coupling, *J. Phys. : Condens. Matter* **29**, 445601 (2017).
  - [16] W. Sacks, T. Cren, D. Roditchev, and B. Douçot, Quasiparticle spectrum of the cuprate  $\text{Bi}_2\text{Sr}_2\text{CaCu}_2\text{O}_{8+\delta}$  : Possible connection to the phase diagram, *Phys. Rev. B* **74**, 174517(2006).
  - [17] W. Sacks, A. Mauger, Y. Noat, Pair-pair interactions as a mechanism for high- $T_c$  superconductivity, *Superconduct. Sci. Technol.*, **28** 105014 (2015).
  - [18] W. Sacks, A. Mauger and Y. Noat, Cooper pairs without glue in high- $T_c$  superconductors : A universal phase diagram, *Euro. Phys. Lett* **119**, 17001 (2017).
  - [19] Yves Noat, Alain Mauger, William Sacks. Superconductivity in cuprates governed by topological constraints. *Physics Letters A* **444**, 128227 (2022).
  - [20] William Sacks, A. Mauger and Y. Noat, Origin of the Fermi arcs in cuprates : a dual role of quasiparticle and pair excitations, *Journal of Physics : Condensed Matter*, **30**, 475703 (2018).
  - [21] R. J. Birgeneau, D. R. Gabbe, H. P. Jenssen, M. A. Kastner, P. J. Picone, T. R. Thurston, G. Shirane, Y. Endoh, M. Sato, K. Yamada, Y. Hidaka, M. Oda, Y. Enomoto, M. Suzuki, and T. Murakami, Antiferromagnetic spin correlations in insulating, metallic, and superconducting

- ting  $\text{La}_{2-x}\text{Sr}_x\text{CuO}_4$  Phys. Rev. B **38**, 6614 (1988).
- [22] L. Krusin-Elbaum, T. Shibauchi, G. Blatter, C.H. Mielke, M. Li, M.P. Maley, P.H.Kes, Pseudogap state in overdoped  $\text{Bi}_2\text{Sr}_2\text{CaCu}_2\text{O}_{8+y}$ , Physica C **387**, Pages 169-174 (2003).
- [23] Maggio-Aprile, I., C. Renner, A. Erb, E. Walker, and Ø. Fischer, Direct vortex lattice imaging and tunneling spectroscopy of flux lines on  $\text{YBa}_2\text{Cu}_3\text{O}_{7-\delta}$ , Phys. Rev. Lett. **75**, 2754 (1995).
- [24] Neel Haldolaarachchige, S. K. Kushwaha, Quinn Gibson and R. J. Cava, Superconducting properties of  $\text{BaBi}_3$ , Supercond. Sci. Technol. **27** 105001 (2014).
- [25] Adel Nader and Pierre Monceau, Critical field of 2H-NbSe<sub>2</sub> down to 50mK, SpringerPlus, **3**, 16 (2014).
- [26] N. Toyota, H. Nakatsuji, K. Noto, A. Hoshi, N. Kobayashi, and Y. Muto and Y. Onodera, Temperature and angular dependences of upper critical fields for the layer structure superconductor 2H-NbSe<sub>2</sub>, Journal of Low Temperature Physics, **25**, Nos. 3/4, 485 (1976).
- [27] Bartłomiej Andrzejewski, Tomasz Klimczuk, Robert J. Cava, The upper critical field in doped  $\text{MgCNi}_3$ , Physica C, Volumes **460-462**, 706 (2007).
- [28] M. Lubell, Empirical scaling formulas for critical current and critical field for commercial NbTi, IEEE Transactions on Magnetics **19**, 754 (1983).
- [29] D.B. Montgomery, H. Wiggall, Measurement of the upper critical field vanadium - gallium alloys, Physics Letters **22**, 48 (1966).
- [30] T. P. Orlando, E. J. McNiff, Jr., S. Foner, and M. R. Beasley, Critical fields, Pauli paramagnetic limiting, and material parameters of  $\text{Nb}_3\text{Sn}$  and  $\text{V}_3\text{Si}$ , Phys. Rev. B **19**, 4545 (1979).
- [31] M. N. Khlopkin, Anisotropy of the upper critical field and specific heat in  $\text{V}_3\text{Si}$  - a superconductor with cubic symmetry, Condensed Matter **69**, 26 (1999).
- [32] S. Foner, E.J. McNiff Jr., B.T. Matthias, T.H. Geballe, R.H. Willens, E. Corenzwit, Upper critical fields of high-temperature superconducting  $\text{Nb}_{1-y}(\text{Al}_{1-x}\text{Ge}_x)_y$  and  $\text{Nb}_3\text{Al}$  : Measurements of  $H_{c2} > 400$  kG at 4.2°K Physics letters. A, **31**, 349 (1970).
- [33] Shaoyan Chu and Michael E. McHenry, Synthesis and superconducting properties of a  $\text{Rb}_3\text{C}_{60}$  single crystal, Phys. Rev. B **55**, 11722 (1997).